A Sparsity Promoting Algorithm for Time of Flight Estimation in Guided Waves - Based SHM

Luca de Marchi, Jochen Moll, Alessandro Marzani

7th European Workshop on Structural Health Monitoring
July 8-11, 2014. La Cité, Nantes, France

A SPARSITY PROMOTING ALGORITHM FOR TIME OF FLIGHT ESTIMATION IN GUIDED WAVES - BASED SHM

Luca De Marchi[1], **Jochen Moll**[2], **Alessandro Marzani**[1]

[1] *DEI-DICAM, University of Bologna, Viale Risorgimento 2, 40136 Bologna, Italy*
[2] *Terahertz Photonics, Goethe University of Frankfurt am Main, Germany*

l.demarchi@unibo.it

ABSTRACT

Ultrasonic Guided Waves (GW) are employed by many Structural Health Monitoring (SHM) systems. In plate-like components, GW based defect detection and localization is typically achieved through multiple piezoelectric transducers arranged in different array configurations. In active methods, one or more actuators are used to generate GWs and the sensors work as wave detectors. Defects can be detected and localized from the wave scattering that they generate. To increase the precision of localization approaches, it is important to minimize the uncertainty in the estimation of the time of flight (ToF) of the waves scattered by the defect. Such task is complicated by the dispersive and multimodal nature of ultrasonic GW propagation. In this work, we analyse two algorithms to extract the ToF from waveforms acquired with a Scanning Laser Doppler Vibrometer (SLDV). The algorithms outputs are used to feed beamforming procedures to image cracks with various orientations.

KEYWORDS : *Guided wave inspections, Dispersion compensation, Scanning Laser Doppler Vibrometer*

INTRODUCTION

The use of Guided Waves (GW) for Structural Health Monitoring (SHM) has interested several researches in the last decades. Detection and localization of defects in plate-like structures by means of Lamb waves has received particular attention [1, 2]. GW are excited and sensed through multiple piezoelectric transducers arranged in different array configurations. In active methods, one or more actuators are used to generate GWs and the sensors work as wave detectors. Defects can be localized from the wave scattering that they generate by adopting classical triangulation procedures. Such procedures are based on the conversion of the waves time-of-flight (ToF) information into distances between sensors and waves reflectors such as plate edges and defects.

To increase the precision of such localization approaches, it is important to minimize the uncertainty in the estimation of the ToF of the wave scattered by the defect. Such task is complicated by the dispersive and multimodal nature of ultrasonic GW propagation. In this work, we analyse two algorithms (A1 and A2) that exploit the concept of frequency warping to extract the ToF.

The first algorithm (A1) for ToF extraction is based on a dispersion compensation procedure [3,4]. Dispersion compensation is achieved with a nonlinear rescaling of the frequency axis (frequency warping). Then, the processed signal envelope is extracted as the absolute value of its Hilbert Transform. Maxima of such envelope are taken as the ToF of waves. The second algorithm (A2) is a sparsity promoting algorithm which minimizes the L1-norm of the acquired signal in a suitable representation basis. In particular, the transducer output can be efficiently represented in Warped Frequency (WF) bases [5], allowing for a very sparse codification of the informative content associated with the acquired waveform. In the new representation, ToF can be extracted from the highest value coefficients. To design the Warped Frequency tools, adopted by both algorithms, the group velocity curves of the

propagating wave modes have to be known. In this work, they were estimated with a semi-analytical finite element (SAFE) formulation [6].

1. PREPROCESSING ALGORITHMS

1.1 Dispersion compensation - A1

As well known, the propagation within certain waveguides such as plates, shells or pipes may be dispersive. That is, the wave group velocity changes with frequencies. This results in a non-linear relation among angular frequency and wavenumber that generates pulse spreading over distance of propagation, complicating thus the estimation of waves ToF. This effect should be somehow compensated to accurately estimate the wave distance of propagation, as typically happens in defect localization procedures. Classical dispersion compensation algorithms are based on a non-linear rescaling (warping) of the frequency axis. The application of such warping procedure to the frequency axis acts so that a linear relation among angular frequency and wavenumber is obtained in the transformed domain (see Figure 1).

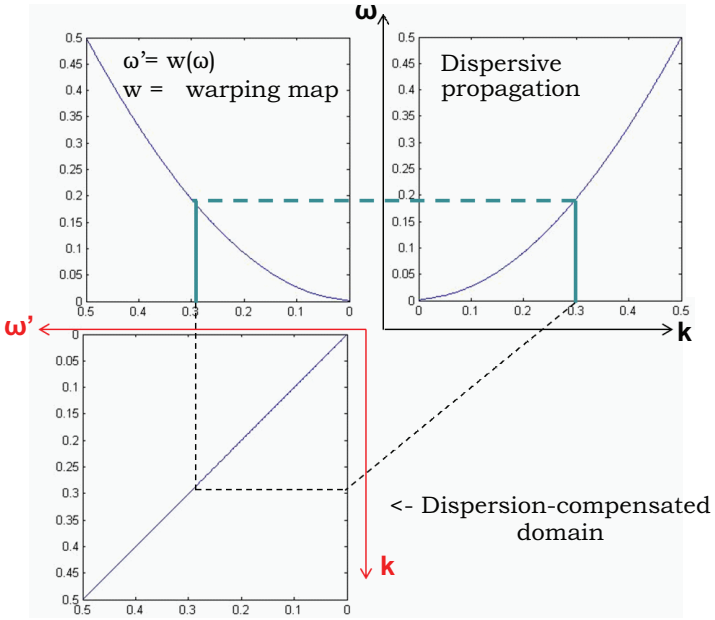

Figure 1 : Dispersion compensation based on the rescaling of the frequency axis

The warping operators have been studied since the early seventies (Warped Frequency Transforms - WFT [7]) and can be computed with fast algorithms based on Fast Fourier Transforms and interpolation procedures. The inverse warping function is defined as the reciprocal of the group velocity $c_g(f)$ of the wave mode whose dispersive effect has to be compensated.

$$K\frac{dw^{-1}(f)}{df} = \frac{1}{c_g(f)} \tag{1}$$

where K is a normalization constant [5]. An undamped guided wave $S(f,D)$ at a traveled distance D from the actuator can be modeled in the frequency domain as dispersive system whose response is given by this formula, which can be rewritten highlighting the relation with inverse warping map:

$$S(f,D) = S_0(f,0)\cdot e^{-j2\pi\int D/c_g(f)df} = S_0(f,0)\cdot e^{-j2\pi w^{-1}(f)KD} \tag{2}$$

where $S_0(f,0)$ is the frequency spectrum of the signal at the actuator (zero distance). The distortion results from the nonlinear phase term $w^{-1}(f)KD$. The warping of the frequency axis ($f' = w(f)$) produces a new waveform whose frequency transform is given by this formula:

$$S(w(f),D) = S_0(w(f),0) \cdot e^{-j2\pi f' KD} \tag{3}$$

It is worth noting that the dispersive effect of the distance is converted in a warped time-delay KD proportional to the distance itself, with a linear dependence of the phase term on the warped frequency f'.

1.2 Basis Pursuit in warped domains - A2

A sparse and high-resolution guided wave signal representation can obtained through a linear decomposition of the acquired signal into a dictionary of basis functions ϕ_γ.

$$s(t) = \sum_{\gamma \in \Gamma} \alpha_\gamma \phi_\gamma \tag{4}$$

where α_γ are real coefficients. In our approach, basis functions are designed to match the spectro-temporal structures of the different propagating GWs by means of the Warped Frequency Transform, and the decomposition method is based on convex optimization (i.e. *Basis Pursuit* [8]), which globally minimizes the L1 norm of the coefficients, thus favouring sparse representations.

Examples of the processing results of the A1 and A2 algorithms are represented in Figure 2. The acquired signal (Fig. 2 (a)) is related to a Lamb wave propagating in an Aluminum plate 1.5mm thick. The effect of WFT processing (A1) is represented in Fig. 2 (b), in this representation the horizontal axis can be directly related to the propagating distance of the wave components. Such processing can be combined to time-gating procedure (Fig. 2 (c)) to isolate the contribution due to defect scattering from the one due to the incident wave or to edge reflected waves, under the assumption that the propagation distance is long enough and the incident wave can be separated in time from the reflections coming from the defect and those from structural elements.

The last plot of this figure (Fig. 2 (d)) represents the signal obtained from the Warped Basis Pursuit (WBP) procedure (A2). Once the values of coefficients α_γ have been found, they are associated to a propagating distance, and re-ordered accordingly [5]. As can be seen, the obtained signal is very sparse and the largest coefficients are concentrated at abscissa values which correspond to the actual distances traveled by the Lamb waves.

2. BEAMFORMING METHODS

Visual inspection of a structural defect requires an image formation procedure that generates two-dimensional maps from the receiver measurements. A conventional method is to use (weighted) beamforming techniques to estimate the position of one or multiple defects. A complimentary technique is given by a model-based approach proposed in [9, 10] where the position of the scatterer results from the solution of a linear system of equations under a sparsity assumption. In this paper, we will consider three different beamforming techniques and feed them with the output of A1 and A2 related to Lamb wave signals actuated with a single PZT and detected by means of scanning Laser Doppler Vibrometer (SLDV). Since only one actuator is used the method suffers from limited aspect angles leading to a circular smearing in the image reconstructions.

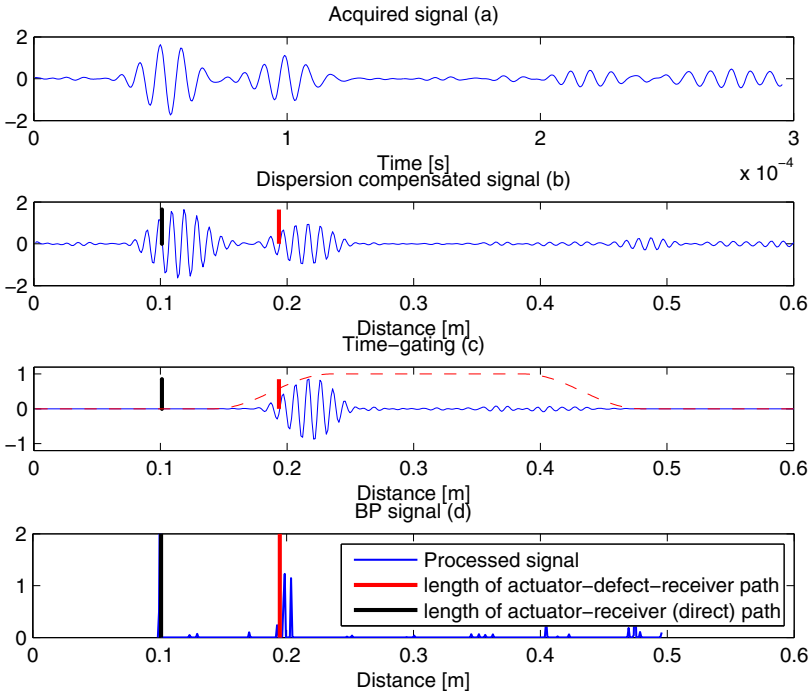

Figure 2 : Processing results of algorithms A1 and A2: (a) Acquired waveform, (b) dispersion compensated signal after the application of A1 to the acquired waveform, (c) dispersion compensated signal after time-gating (the dashed line represents the applied time-window), (d) output of A2

2.1 Delay-and-sum beamforming (DAS)

The basic Delay-and-Sum (DAS) algorithm used e.g. in [11] uniformly superimposes the images of each actuator-sensor-combination to form a two-dimensional intensity map. The index of the actuator is given here by $i \ldots N_A$ and that of the receiver by $j \ldots N_S$. The DAS-method can be expressed as:

$$I(\vec{x}) = \sum_{i=1}^{N_A} \sum_{j=1}^{N_S} w_{ij}(\vec{x}) \cdot s_{ij}(t - \tau_{ij}) \tag{5}$$

where the weighting of each channel is equally $w_{ij}^{\mathrm{DAS}}(\vec{x}) = 1$. The receiver signal is given by $s_{ij}(\cdot)$ and the time-delay by τ_{ij}. Similar to all other beamforming techniques, the DAS-method requires the group velocity c_g to transform the time-traces linearly from time to range-domain. This transformation is realized in this paper by a pre-processing step using either method A1 or A2.

2.2 Weighted beamforming using the coherence factor method (CF)

The coherence factor method enables data-adaptive focusing through a spatial coherence quality of the measured signals: the better the signals of all sensor-pairs coherently sum up at a given voxel $\vec{x}$ the more this voxel is weighted [12]. The image formation given by Equation (5) uses a weighting called the coherence factor $w_{ij}^{\mathrm{CF}}(\vec{x})$:

$$w_{ij}^{\mathrm{CF}}(\vec{x}) = \frac{\left| \sum_{i=1}^{N_A} \sum_{j=1}^{N_S} s_{ij}(t - \tau_{ij}) \right|^2}{N_A \cdot N_S \cdot \left(\sum_{i=1}^{N_A} \sum_{j=1}^{N_S} \left| s_{ij}(t - \tau_{ij}) \right|^2 \right)} \tag{6}$$

By definition the weighting factor lies between 0 and 1.

2.3 Channel-ranked beamforming technique (RANK)

Another modified DAS-algorithm presented in [13] is called channel-ranked beamforming technique. For a given focal voxel and a particular actuator-sensor pair, a propagation distance $r_{ij}(\vec{x})$ is mapped to each signal. Longer propagation distances are generally more affected to distortions than shorter ones. Therefore, this method weights channels with shorter propagation distances stronger for each voxel:

$$w_{ij}^{\mathrm{RANK}}(\vec{x}) = \frac{rank_{ij}(\vec{x})}{N \cdot (N+1)/2} \tag{7}$$

where $rank_{ij}(\vec{x})$ is a linear ordering from $1,2,3,\ldots,N$ with 1 assigned to the longest propagation distance.

3. RESULTS

The experiment is conducted on a 1.5 mm thick aluminum plate whose dimensions are 540 mm x 540 mm. A 10 mm diameter PZT transducer was bonded at the center of the plate and 4 through cracks each 30 mm long were introduced. The cracks have different orientation with respect to the actuator position and hence to the incident wavefield. The acoustic wavefield was generated by exciting a short sinusoidal burst with a PZT transducer, and recorded by a Scanning Laser Doppler Vibrometer (SLDV) over the whole plate area. In Fig. 3, a snapshot of the SLDV imaging is plotted. It is worth noting how the incident wave is scattered by the different cracks. A subset of the acquired waveforms was then selected (200 signals), to mimic the behavior of an array of piezoelectric sensors.

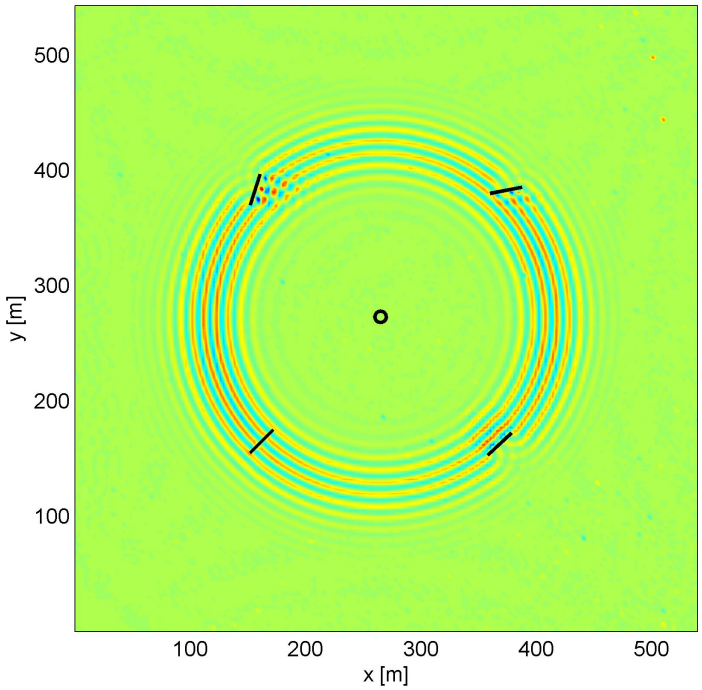

Figure 3 : A snapshot of the acquired wavefield.

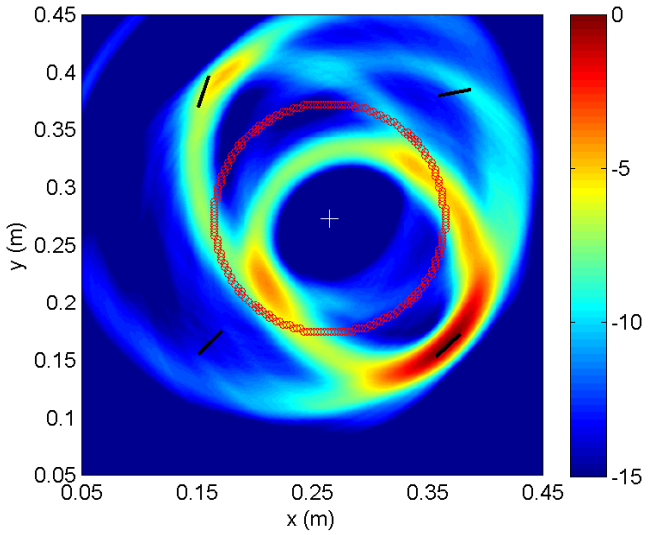

Figure 4 : Defect imaging obtained by processing the dispersion compensated signals (A1 algorithm) with DAS beamforming.

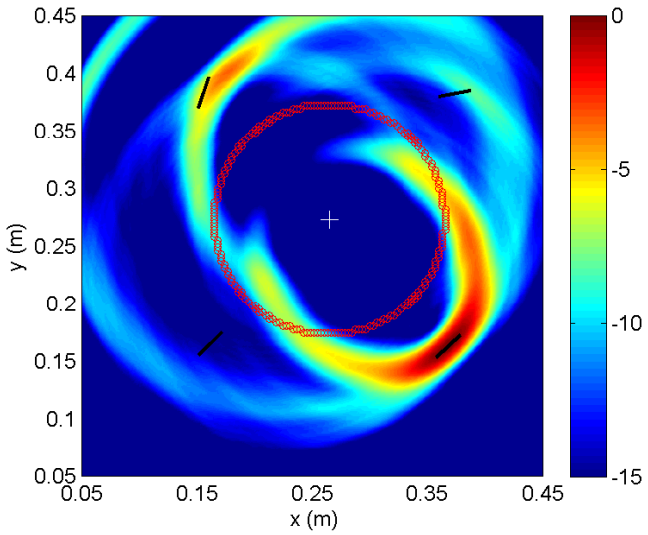

Figure 5 : Defect imaging obtained by processing the dispersion compensated signals (A1 algorithm) with RANK beamforming.

Such waveforms were processed with A1 and A2, and then with the beamforming techniques mentioned in the previous section. The results can be qualitatively evaluated by looking at Fig. 4, 5, 6 and 7. In these figures, the circles correspond to the selected recording points within the scan area. It is worth noticing that all the considered imaging procedures are baseline free, that is we didn't exploit information about the pristine structure to highlight the presence of defects. Hence, there is no temperature compensation technique required as demonstrated e.g. in [14]. It is worth noticing that this approach is valid for isotropic structures, but may generate a systematic error for fiber reinforced media (as shown e.g. in [15]), where the group velocity is directional according to the orientation of the fibers. As further developments, we plan to extend the considered processing to such anisotropic structures.

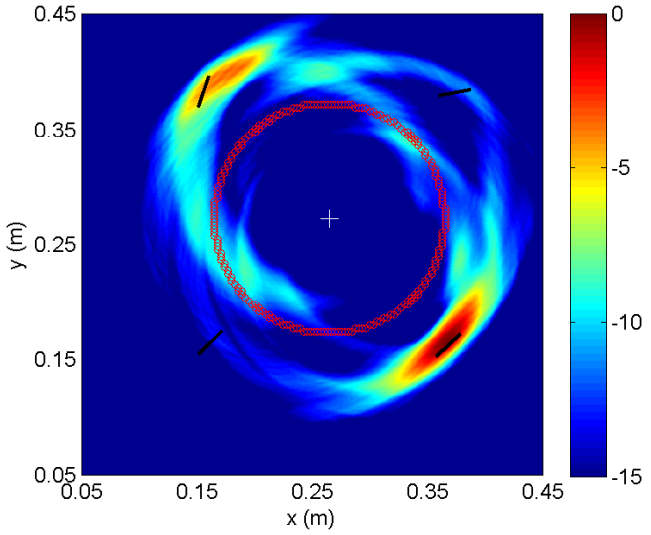

Figure 6 : Defect imaging obtained by processing the dispersion compensated signals (A1 algorithm) with CF beamforming.

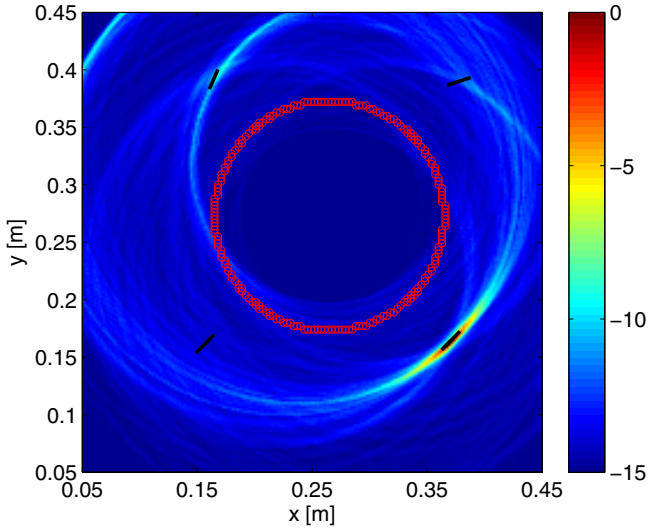

Figure 7 : Defect imaging obtained by processing the WBP signals (A2 algorithm) with DAS beamforming.

CONCLUSION

Among the two algorithms evaluated for ToF estimation, the one based on the sparsity promoting representations minimizes the ToF estimation uncertainty and produces a highly resolved defect imaging. Despite this, it was not possible to image the defect oriented at 90^o w.r.t. to the incident wave front since the scattered energy is too weak compared to the incident one. Optimized and adaptive selection of the receiver array shape, size, and weights is under investigation to further improve accuracy of the investigated approach, and to extend its applicability to anisotropic structures.

ACKNOWLEDGEMENTS

The authors thank Prof. Fritzen (University of Siegen, Germany) for providing the SLDV. The research leading to these results has received funding from the SARISTU project (Grant Agreement no. 284562).

REFERENCES

[1] S. Hurlebaus, M. Niethammer, L. J. Jacobs, and C. Valle. Automated methodology to locate notches with Lamb waves. *Acoustic Research Letters Online*, 2(4), 2001.

[2] A. Raghavan and C.E.S. Cesnik. Guided-wave signal processing using chirplet matching pursuits and mode correlation for structural health monitoring. *Smart Materials and Structures*, 16(2):355, 2007.

[3] PD Wilcox. A rapid signal processing technique to remove the effect of dispersion from guided wave signals. *IEEE Transactions on Ultrasonics, Ferroelectrics and Frequency Control*, 50(4):419–427, 2003.

[4] René Sicard, Jacques Goyette, and Djamel Zellouf. A numerical dispersion compensation technique for time recompression of lamb wave signals. *Ultrasonics*, 40(1):727–732, 2002.

[5] Luca De Marchi, Massimo Ruzzene, Buli Xu, Emanuele Baravelli, and Nicolo Speciale. Warped basis pursuit for damage detection using lamb waves. *Ultrasonics, Ferroelectrics and Frequency Control, IEEE Transactions on*, 57(12):2734–2741, 2010.

[6] P. Bocchini, A. Marzani, and E. Viola. Graphical user interface for guided acoustic waves. *Journal of Computing in Civil Engineering*, 25(3):202–210, 2011.

[7] Alan V Oppenheim and Donald H Johnson. Discrete representation of signals. *Proceedings of the IEEE*, 60(6):681–691, 1972.

[8] S. S. Chen, D. L. Donoho, and M. A. Saunders. Atomic Decomposition by Basis Pursuit. *SIAM Rev.*, 43(1):129–159, 2001.

[9] R.M. Levine and J.E. Michaels. Model-based imaging of damage with lamb waves via sparse reconstruction. *Journal of the Acoustical Society of America*, 133(3):1525–1534, 2013.

[10] C. Kexel, J. Moll, M. Kuhnt, F. Wiegandt, and V. Krozer. Compressed sensing for three-dimensional microwave breast cancer imaging. In *8th European Conference on Antennas and Propagation*, pages 1634–1638, 2014.

[11] Jennifer E Michaels, Anthony J Croxford, and Paul D Wilcox. Imaging algorithms for locating damage via in situ ultrasonic sensors. In *Sensors Applications Symposium, 2008. SAS 2008. IEEE*, pages 63–67. IET, 2008.

[12] M. Klemm, J. Leendertz, D. Gibbins, I.J. Craddock, A. Preece, and R. Benjamin. Microwave radar-based breast cancer detection: Imaging in inhomogeneous breast phantoms. *IEEE Antennas and Wireless Propagation Letters*, 8:1349–1352, 2009.

[13] M. O'Halloran, M. Glavin, and E. Jones. Channel-ranked beamformer for the early detection of breast cancer. *Progress In Electromagnetics Research*, 103:153–168, 2010.

[14] J Moll and CP Fritzen. Guided Waves for Autonomous Online Identification of Structural Defects under Ambient Temperature Variations. *Journal of Sound and Vibration*, 331(20):4587–4597, 2012.

[15] J. Moll, RT Schulte, B. Hartmann, C.-P. Fritzen, and O. Nelles. Multi-site damage localization in anisotropic plate-like structures using an active guided wave structural health monitoring system. *Smart Materials and Structures*, 19(4):045022, 2010.